Tzu Chi Medical Journal 2021; 33 (1): 42–48

Original Article

Effects of different electrodes used in bone-guided extracochlear implants on electrical stimulation of auditory nerves in guinea pigs

*Chien-Hao Liu[a], Yung-Shan Lu[a], Po-Chun Chen[b], Chia-Fone Lee[c,d]**

[a]Department of Mechanical Engineering, National Taiwan University, Taipei, Taiwan, [b]Department of Materials and Mineral Resource Engineering, Institute of Materials Science and Engineering, National Taipei University of Technology, Taipei, Taiwan, [c]Department of Otolaryngology, Hualian Tzu Chi Hospital, Buddhist Tzu Chi Medical Foundation, Hualien, Taiwan, [d]Department of Otolaryngology Head and Neck Surgery, School of Medicine, Tzu Chi University, Hualien, Taiwan

Submission : 23-Mar-2020
Revision : 20-Apr-2020
Acceptance : 08-May-2020
Web Publication : 13-Jul-2020

Abstract

Objective: Conventional cochlear implants provide patients who are deaf with hearing via electrical intracochlear stimulations. Stimulation electrodes are inserted into the cochlea through a cochleostomy or round window membrane (RWM) approach. However, these methods might induce cochlear ossificans and loss of residual hearing by damaging inner ear structures. To avoid an invasive electrode insertion, we developed a novel bone-guided extracochlear implant that stimulated the auditory nerves between the cochlear bones and the RWM to prevent cochlea damage. Power consumption plays an important role in wireless implantable electronic devices. Therefore, we aimed to investigate the effects of different electrodes on the stimulating threshold currents of the auditory nerve and the power consumption of bone-guided extracochlear implants using a commercial stimulator. **Materials and Methods:** Inert aurum (Au) electrodes were compared with biocompatible platinum (Pt) and iridium oxide (IrO_x) electrodes in practical implantable applications. IrO_x electrodes were used for their high-charge storage capacity, low impedance, and biocompatibility. The electrodes were fabricated via sputtering and were experimentally characterized with cyclic voltammetry and then examined using *in vivo* tests. **Results:** Based on electrical auditory brainstem responses, IrO_x electrodes yielded lower acoustic nerve-stimulating threshold currents (132 μA) compared with Au electrodes (204 μA). IrO_x electrodes also had a lower acoustic nerve stimulating threshold current (132 μA) compared with Pt electrodes (168 μA). **Conclusion:** As expected, IrO_x electrodes were beneficial in the development of multielectrode bone-guided extracochlear implants, with the lowest acoustic nerve-stimulating threshold and current consumptions compared with Au and Pt electrodes.

Keywords: *Current consumption, Cyclic voltammetry, Implantable electronics, Iridium oxide electrode, Stimulation threshold*

Introduction

Cochlear implants have been used extensively during the past few decades to provide an electronic sense of sound to patients who are deaf and to those who are hearing impaired via acoustic nerve electrical stimulation [1-5]. In general, a cochlear implant is composed of external audio signal processing, wireless communication, and implanted units, including a signal-processing device, a stimulator, and an electrode array. The sounds acquired through the microphone of the external unit are encoded into modulated electrical signals and transmitted wirelessly to the implanted unit. The electrical signals are then converted to a series of pulse stimuli applied to the electrode array. The electrode array, comprised multiple electrodes arranged along the cochlear axis, is surgically inserted into the cochlea. When the electrical pulse signals are applied to different electrodes, the auditory nerves corresponding to different frequencies at the basilar membrane are activated, and the evoked action potentials are transferred to the brain to interpret the sounds. Although cochlear implants involve well-established techniques, several studies have aimed to improve their performance, using thin-film curl electrodes; piezoelectric, microelectromechanical-based, or microphone implants; transmission antennas; advanced signal-processing or filtering algorithms; bilateral cochlear implants; optical cochlear implants; and combined hearing aids with cochlear implants [6-19]. For example, a general electrode array contains 8–24 electrodes and cannot match all the auditory

Access this article online
Quick Response Code:
Website: www.tcmjmed.com
DOI: 10.4103/tcmj.tcmj_46_20

**Address for correspondence:*
Dr. Chia-Fone Lee,
Department of Otolaryngology, Hualian Tzu Chi Hospital, Buddhist Tzu Chi Medical Foundation, 707, Section 3, Chung-Yang Road, Hualien, Taiwan.
E-mail: e430013@yahoo.com.tw

How to cite this article: Liu CH, Lu YS, Chen PC, Lee CF. Effects of different electrodes used in bone-guided extracochlear implants on electrical stimulation of auditory nerves in guinea pigs. Tzu Chi Med J 2021; 33(1): 42-8.

nerves; therefore, it cannot cover the entire frequency band of audible frequencies [1]. To improve frequency resolution, several techniques have been reported such as current steering, fine structures, and electric-field focusing [20-23]. Moreover, advanced signal-processing approaches and filtering algorithms have also been used to enhance speech recognition [24]. However, cochlear implants are associated with disadvantages such as complicated surgical procedures (through the round window membrane [RWM] or via a cochleostomy), risk of meningitis, cochlear ossificans, and the possible loss of residual hearing owing to the insertion of an electrode array inside the cochlea [17]. Therefore, conventional cochlear implants are suitable for patients with a profound hearing disability. In a previous study, we reported that a complementary metal-oxide semiconductor (CMOS)-based bone-guided extracochlear implant could electrically stimulate the basal regions of the cochlea and simultaneously preserve part of the residual hearing. To avoid inserting electrodes into the cochlea, electrode arrays were placed between the cochlear bones and the RWM [25], and electrical stimulating signals were transmitted via the cochlear bones to activate auditory nerves in the basilar membrane.

Power consumption is an important issue for wireless implantable electronic devices. For example, commercially available cochlear implants require frequent battery replacement to provide sufficient power for wireless communication, signal processing, and electrical stimulations. For most cochlear implants, stimulators produce biphasic or monophasic stimulation currents, with an amplitude ranging from 10 μA to 2 mA and require a power link budget of 20–40 mW [1]. The power transmission can be reduced via optical wireless cochlear implants that consume within μW [14]. In contrast, the proposed bone-guided extracochlear implant requires a relatively large power input for stimulation through the cochlear bones. In this study, we investigated the use of inert metals, due to research budget limitations.

Aurum (Au) was used in our preliminary studies to synthesize the stimulating electrodes. The minimum stimulating threshold current approximately ranged from 200 to 300 μA for Au-based electrodes to activate the acoustic nerves. However, Au ions can be potentially leached and cause electrode delamination and are not suitable, therefore, for long-term usage and implantable applications. Furthermore, the stimulating electrodes can profoundly affect activation of the acoustic nerves for bone-guided extracochlear implants and in terms of power consumption. In this study, we aimed to investigate two well-known biocompatible electrodes, namely, platinum (Pt) and iridium oxide (IrO_x), to determine their practical implantable applications. IrO_x electrodes have previously been used in bone-guided extracochlear implants owing to their high conductivity, chemical stability, and low electrochemical impedance properties, which have been shown to lead to lower threshold currents and low input power supply levels [26,27]. To investigate the effects of the electrodes on bone-guided extracochlear implants, these electrodes were fabricated via standard photolithographic processes and were

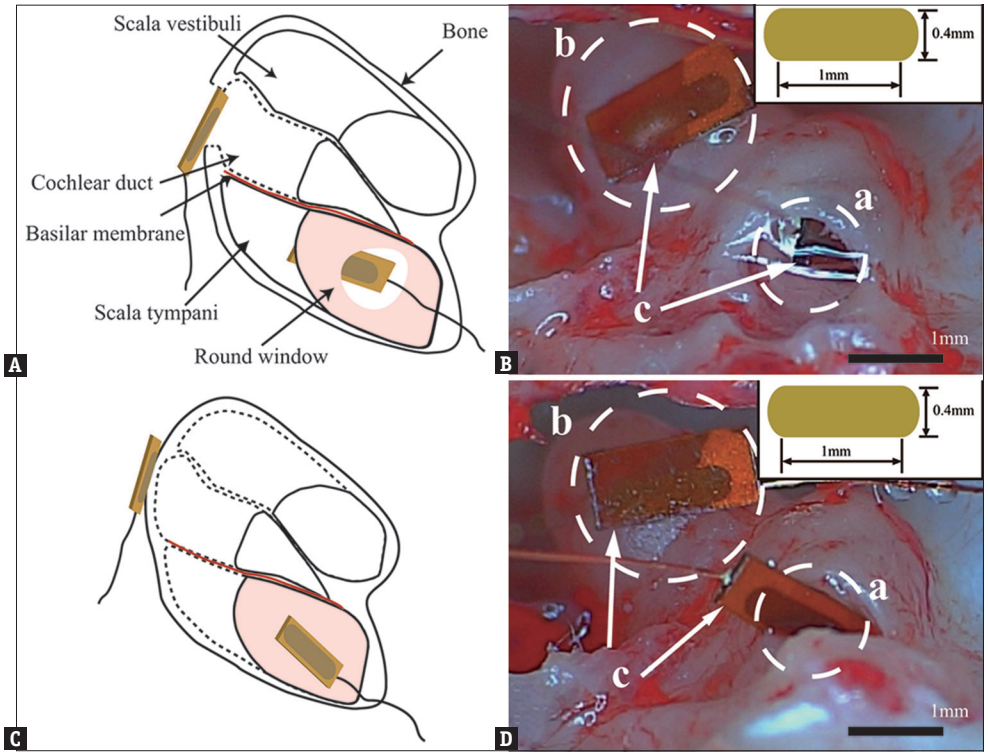

Figure 1: (A) Illustrations of intracochlear stimulation in cases where the electrode array was inserted inside the cochlea; (B) electrode arrangements in which one electrode was inserted through the round window membrane and the other was placed into the cochlea; (C) bone-guided extracochlear stimulation: Electrodes were placed between the outer surfaces of the round window membrane and cochlea bones, and; (D) one electrode was placed on the outer surface of the round window membrane and the other electrode was placed on the outer surface of the cochlear bones. (a) The round window, (b) the cochlear bone, and (c) the electrodes

examined experimentally using *in vivo* tests involving guinea pigs. To simplify the experimental setup and animal tests, we substituted the CMOS-based stimulator with a commercial stimulator that had been used in preliminary studies.

In this study, we introduce the mechanism of bone-guided extracochlear stimulation. We present the fabrication processes for Pt and IrO_x electrodes and characterize the electrode properties experimentally. Subsequently, these electrodes are used for bone-guided extracochlear stimulation and are examined using *in vivo* tests to determine the stimulating acoustic nerve threshold currents, following which we summarize our results.

Materials and methods

In vivo tests

The guinea pigs used for the animal tests were bred at the National Taiwan University College of Medicine and the College of Public Health. The study was approved by the Institutional Animal Care and Use Committee of the National Taiwan University College of Medicine and the College of Public Health (approval number 20150008) on February 2, 2015. For the animal tests, 20 guinea pigs were anesthetized with sodium pentobarbital (30 mg/kg of body weight). To maintain anesthesia throughout the experiments, a dose of 10 mg/kg body weight was injected into the guinea pigs whenever they showed signs of increased arousal, based on observations of a paw withdrawal reflex test undertaken every 30 min. To implant the electrodes, surgery was conducted to open the bulla to facilitate electrode installation. In this study, we examined two different stimulation approaches, namely, (a) intracochlear stimulations and (b) our proposed bone-guided extracochlear stimulation, as shown in Figure 1.

Acoustic stimulations

The hearing capacities of the tested animals were examined before the electrical stimulations. A 120 dB click sound pressure level (SPL) was delivered into the ears of the guinea pigs through silicon tubes via an auditory brainstem response (ABR).

Intracochlear stimulations

Two electrodes were inserted inside the cochlea to activate the auditory nerves, one was placed directly into the cochlea through the cochleostomy opening and the other through a small hole in the RWM, as shown in Figure 1a. Electrical ABRs (eABRs) were measured using the acquisition part of the ABR system (IHS, Intelligent Hearing System; Model Opti–Amp8002). The recording parameters were as follows: stimulation rate, 25 stimulus per second; 100 Hz to 3 kHz bandpass filters; amplification gain, 100 K; and analysis time window, 12 ms. The click sound was used for acoustic stimulation. The signal was triggered using the ABR system and sent to the pulse stimulator (A-M system: Isolated pulse stimulator model 21). The electric pulses were generated using the A-M system and connected to the electrodes. The nerve response was recorded using the ABR system [25].

Bone-guided extracochlear stimulations

In bone-guided extracochlear stimulations, the electrodes were placed on the surfaces between the RWM and the cochlear bones, as shown in Figure 1c. In addition, the auditory nerves were also excited via extracochlear stimulations. Based on our previous finite element model and on analysis using guinea pigs, it has been shown that electrical fields can cross through the basilar membrane and the peripheral auditory nerve fibers [28,29]. Figure 1d shows images of the proposed bone-guided extracochlear stimulation, based on the placement of one of the electrodes on the outer part of the RWM and the other electrode placed on the surface of the cochlear bone.

The experimental setup concerning the *in vivo* animal tests used to study the effects of the electrodes on the bone-guided extracochlear stimulation is described.

Electrode fabrication

The implantable electrodes were designed and fabricated on polyimide substrates. Figure 2a-c illustrates the fabrication processes of the implantable electrodes. The polyimide substrate was cleaned prior to the photolithography process with acetone, isopropanol, DI water, and oxygen plasma. AZ5214–E was utilized as a photoresist to define the electrode dimensions. The electrode size used in this study was 1 mm × 0.4 mm. The polyimide was coated with tantalum as an adhesive layer. Au, Pt, and IrO_x were then deposited on the top of the adhesive layer using optimum sputtering conditions. After the sputtering processes, AZ5214–E was removed using acetone at 30°C. Finally, the electrodes were cut and connected to a copper wire using silver paste.

The surface morphologies of the fabricated and postimplanted electrodes were observed using scanning electron microscopy (SEM, JEOL JSM–6510 LV) and scanning probe microscopy (SPM, Bruker Innova). The charge storage capacity (CSC) of the Au, Pt, and IrO_x electrodes was determined using a cyclic voltammetry scan (CV), with voltages in the range of 0.6–0.8 V at 50 mV/s in 1× phosphate buffer saline (Corning). In addition, the reference and counter electrodes were made of Ag/AgCl and Pt wires, respectively. Figure 2d and e shows the SEM images of the IrO_x electrodes. A high-resolution image at a magnification of 10^5 revealed granular morphology with a refined surface texture for the IrO_x electrodes. The SPM image indicated that the roughness of the IrO_x was 4.81 nm. As a result, the IrO_x electrode was successfully fabricated using our designed process.

Characterizations of electrodes

Figure 3 shows the CSC profiles from the 20^{th} cycle of the CV experiments for various samples at 50 mV/s. Our CSC profiles from the IrO_x electrode were consistent with those previously reported in which oxidation/reduction peaks appeared. The corresponding CSC values for Au, Pt, and IrO_x electrodes were 0.61 mC/cm^2, 1.43 mC/cm^2, and 15.92 mC/cm^2, respectively. The IrOx electrode demonstrated a higher CSC value. In Figure 2, SEM images of the as deposit [Figure 2f h] and postimplanted [Figure 2i k] Au, Pt, and IrOx electrodes are shown. As observed in these SEM images, the electrodes remained intact after conducting *in vivo* electrical stimulations.

Results

The hearing capacities of the tested animals were examined prior to the electrical stimulations. Figure 4a shows the

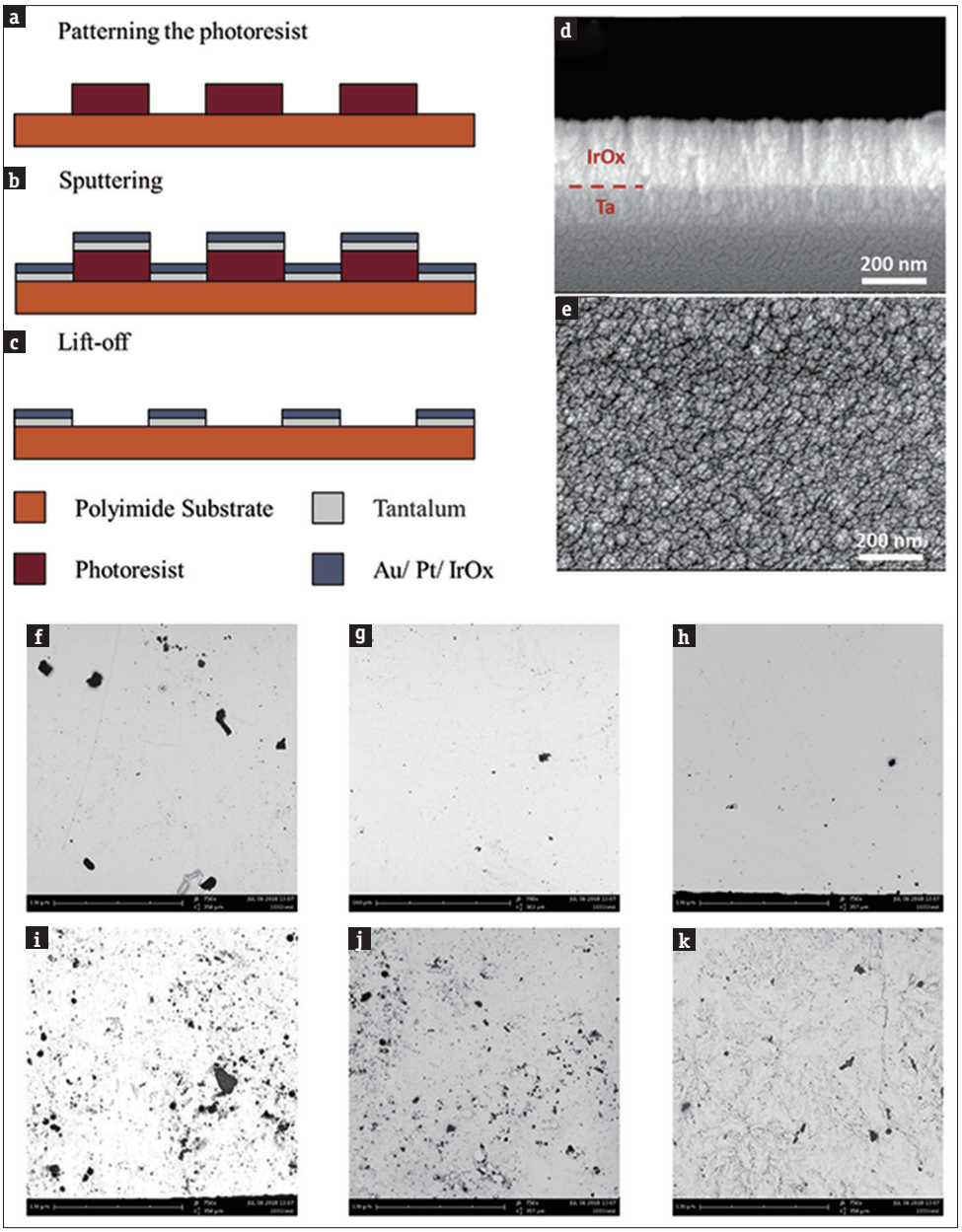

Figure 2: (a-c) Schematic of the electrode preparation process. Scanning electron microscopy images of the iridium oxide electrode in (d) cross-sectional and (e) planar views. Corresponding scanning electron microscopy images of the as-deposit (f-h) and postimplanted (i-k) aurum, platinum, and iridium oxide electrodes

measured, acoustic ABR signals following stimulations with click sounds at a SPL of 120 dB [25]. The evoked waveforms I to IV indicated that the tested animals had a regular auditory ability. Figure 4b shows the eABR signals using a current of 500 μA, based on intracochlear stimulations described in Figure 1a. Figure 4c shows the received eABR signals evoked with a stimulating current of 500 μA following extracochlear stimulations, as shown in Figure 1c. The measured IV waveforms indicated the activations of the auditory nerve. The wave morphology and latency of the eABR of the acoustic nerves between the intracochlear and extracochlear stimulations were similar. These results indicated that biphasic electric stimulations of bone-guided extracochlear stimulations could successfully activate the acoustic nerve. To investigate the stimulating nerve threshold currents, the stimulating currents were altered from 100 to 500 μA. Figure 4d shows a biphasic waveform of the stimulating current with a pulse period of 200 μs and a tunable amplitude. Figure 4e shows the measured ABR signals evoked at different stimulation currents ranging from 100 to 500 μA, where the peak of wave IV could be exploited to determine the occurrences of the successful stimulations of the auditory nerves. In cases where the auditory nerves were activated, the amplitude of the evoked IV waveform (i.e., the potential of the evoked wave IV relative to zero potential) was larger than 0.3 μV. The experiments described above were repeated using three different electrodes. The wave form of the eABR signal in Figure 4e was within the threshold mode (sweep = 50) and

the amplitudes were within the stack. The wave form of eABR signals in Figure 4b using intracochlear stimulation and Figure 4c using extracochlear stimulation was within the normal neuronal response record modes (sweep = 250); therefore, some difference was apparent. The stimulation rates were the same (rate: 25/sec).

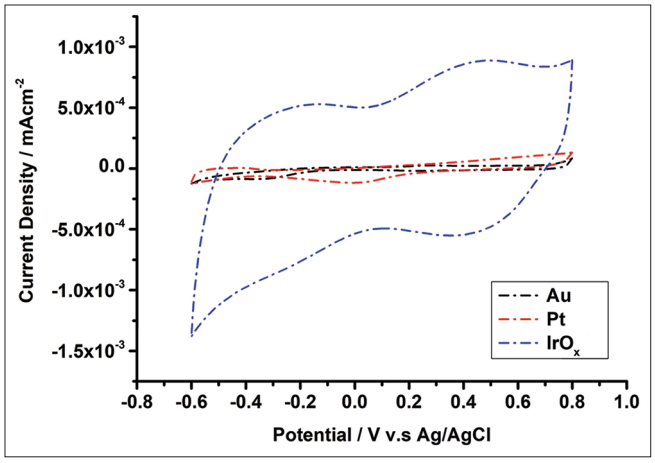

Figure 3: Cyclic voltammetry curve of the fabricated aurum, platinum, and iridium oxide electrodes

Current thresholds of acoustic nerve

Through gradually increasing the stimulating currents from 100 to 500 μA, as shown in Figure 4e, the threshold could be determined based on the occurrences of the evoked wave IV. Figure 5 shows the static distributions of the threshold currents for different electrodes comprised Au, Pt, and IrO_x, based on different experiments, with error bars indicating the standard deviations.

Discussion

The results of extracochlear stimulations presented in Figure 5 show that the IrO_x electrode had the lowest averaged auditory nerve-stimulating threshold currents compared with the other electrodes because IrO_x had a high-CSC. Although the deviations were relatively large, the averaged stimulation threshold trends demonstrated that IrO_x yielded the lowest stimulating threshold currents. IrO_x-based electrodes could activate auditory nerves with the lowest stimulating currents. Our results indicated that stimulating currents with lower thresholds could significantly reduce the required input supply power. This effect could potentially assist a battery to operate for a greater length of time. To achieve an increased frequency resolution, multiple electrode arrays should be further developed in bone-guided extracochlear implants to provide multichannel stimulations,

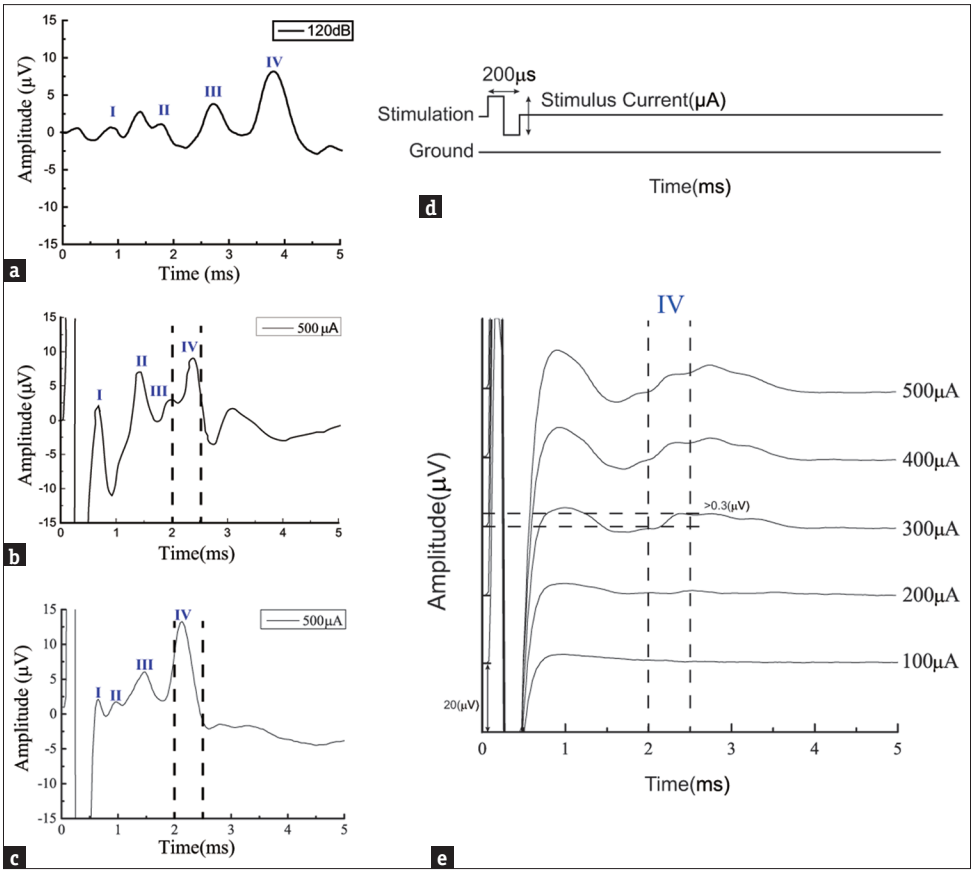

Figure 4: (a) Evoked acoustic auditory brainstem response signals with 120 dB SPL. The evoked waveforms I to IV indicated that the tested animal had a regular auditory ability; (b) received electrical auditory brainstem response signals intracochlear stimulation current of 500 μA, as shown in (a); (c) received electrical auditory brainstem response signals following extracochlear stimulation with a current of 500 μA, as shown in (c); (d) biphasic waveform of the stimulation current with a period of 200 μs and a tunable amplitude, and; (e) evoked electrical auditory brainstem response signals at different stimulation currents ranging from 100 to 500 μA for the determination of the threshold currents

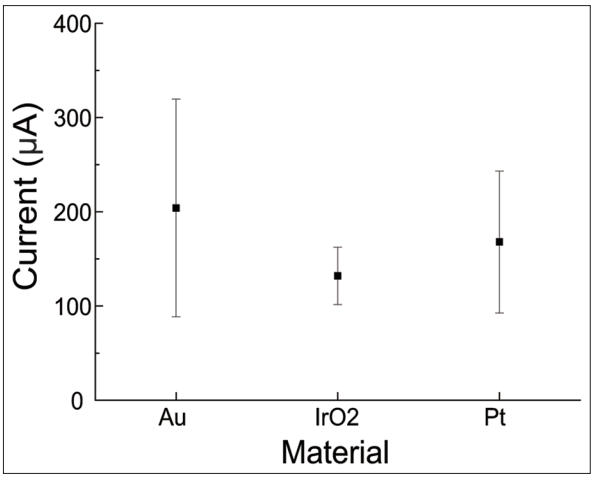

Figure 5: Were the results of extracochlear stimulation. Static distributions of the threshold currents for different electrodes composed of aurum, platinum, and iridium oxide were based on different experiments. Error bars corresponded to the standard deviations. The iridium oxide electrode yielded threshold currents with the lowest averages, indicating that auditory nerves could be activated with low stimulating currents

and we intend to conduct further investigations in future studies. We anticipate that the IrO_x electrode that showed the lowest stimulation threshold is likely to be beneficial in developing multielectrode arrays for bone-guided extracochlear stimulations compared with Au and Pt electrodes.

Conclusion

In this study, we investigated the effects of different electrodes on stimulating acoustic nerve threshold currents and power consumption for bone-guided extracochlear stimulations. We compared the inert Au electrode, which our group had developed previously, with two other well-known biocompatible Pt and IrO_x electrodes. These electrodes were fabricated with standard lithographic techniques and were experimentally examined with *in vivo* tests. Our findings showed that the auditory nerves at the basilar membrane could be stimulated and activated via the IrO_x electrodes at the lowest activating nerve threshold currents compared with the other electrodes through bone-guided extracochlear stimulation. The IrO_x electrodes could reduce the required power supply input of the CMOS-based bone-guided extracochlear implants developed in our previous work. Therefore, lower stimulating thresholds might increase battery lifetime. These study findings are likely to be beneficial for the development of multichannel and multiple electrode arrays for bone-guided extracochlear implants.

Financial support and sponsorship

Nil.

Conflicts of interest

There are no conflicts of interest.

References

1. Agarwal K, Jegadeesan R, Guo YX, Thakor NV. Wireless Power Transfer Strategies for Implantable Bioelectronics. IEEE Rev Biomed Eng 2017;10:136-61.
2. Choi CT, Wang SP. Modeling ECAP in cochlear implants using the FEM and equivalent circuit. IEEE Trans Magn 2014;50:49-52.
3. Gao X, Grayden DB, McDonnell MD. Modeling electrode place discrimination in cochlear implant stimulation. IEEE Trans Biomed Eng 2017;64:2219-29.
4. Watanabe H, Velmurugan J, Mirkin MV, Svirsky MA, Lalwani AK, Llinas RR. Scanning electrochemical microscopy as a novel proximity sensor for atraumatic cochlear implant insertion. IEEE Trans Biomed Eng 2014;61:1822-32.
5. Yang G, Lyon RF, Drakakis EM. A 6 μW per channel analog biomimetic cochlear implant processor filterbank architecture with across channels AGC. IEEE Trans Biomed Circuits Syst 2015;9:72-86.
6. Buyens W, Dijk B van, Wouters J, Moonen M. A stereo music preprocessing scheme for cochlear implant user. IEEE Trans Biomed Eng. 2015;62:2434-42.
7. Hillman T, Badi AN, Normann RA, Kertesz T, Shelton C. Cochlear nerve stimulation with a 3-dimensional penetrating electrode array. Otol Neurotol 2003;24:764-8.
8. Johnson AC, Wise KD. An active thin-film cochlear electrode array with monolithic backing and curl. J Microelectromech Syst 2014;23:428-37.
9. Koning R, Madhu N, Wouters J. Ideal time-frequency masking algorithms lead to different speech intelligibility and quality in normal-hearing and cochlear implant listeners. IEEE Trans Biomed Eng 2015;62:331-41.
10. Litovsky RY, Parkinson A, Arcaroli J, Peters R, Lake J, Johnstone P, et al. Bilateral cochlear implants in adults and children. Arch Otolaryngol Head Neck Surg 2004;130:648-55.
11. Moser T. Optogenetic stimulation of the auditory pathway for research and future prosthetics. Curr Opin Neurobiol 2015;34:29-36.
12. Paun MA, Paun VA. High-frequency 3-D model for the study of antennas in cochlear implants. IEEE Trans Compon Packag Manuf Technol 2018;8:1135-40.
13. Pfiffner F, Prochazka L, Peus D, Dobrev I, Dalbert A, Sim JH, et al. A MEMS condenser microphone-based intracochlear acoustic receiver. IEEE Trans Biomed Eng 2017;64:2431-8.
14. Trevlakis SE, Boulogeorgos AA, Sofotasios PC, Muhaidat S, Karagiannidis GK. Optical wireless cochlear implants. Biomed Opt Express 2019;10:707-30.
15. Turner CW, Reiss LA, Gantz BJ. Combined acoustic and electric hearing: Preserving residual acoustic hearing. Hear Res 2008;242:164-71.
16. van Hoesel RJ, Tyler RS. Speech perception, localization, and lateralization with bilateral cochlear implants. J Acoust Soc Am 2003;113:1617-30.
17. von Ilberg C, Kiefer J, Tillein J, Pfenningdorff T, Hartmann R, Stürzebecher E, et al. Electric-acoustic stimulation of the auditory system. New technology for severe hearing loss. ORL J Otorhinolaryngol Relat Spec 1999;61:334-40.
18. Wong P, George S, Tran P, Sue A, Carter P, Li Q. Development and validation of a high-fidelity finite-element model of monopolar stimulation in the implanted guinea pig cochlea. IEEE Trans Biomed Eng 2016;63:188-98.
19. Xu Y, Luo C, Zeng FG, Middlebrooks JC, Lin HW, You Z. Design, fabrication, and evaluation of a parylene thin-film electrode array for cochlear implants. IEEE Trans Biomed Eng 2019;66:573-83.
20. Arenberg JG, Parkinson WS, Litvak L, Chen C, Kreft HA, Oxenham AJ. A dynamically focusing cochlear implant strategy can improve vowel identification in noise. Ear Hear 2018;39:1136-45.
21. Buechner A, Brendel M, Krüeger B, Frohne-Büchner C, Nogueira W, Edler B, et al. Current steering and results from novel speech coding strategies. Otol Neurotol 2008;29:203-7.
22. Landsberger DM, Padilla M, Srinivasan AG. Reducing current

spread using current focusing in cochlear implant users. Hear Res 2012;284:16-24.

23. Magnusson L. Comparison of the fine structure processing (FSP) strategy and the CIS strategy used in the MED-EL cochlear implant system: Speech intelligibility and music sound quality. Int J Audiol 2011;50:279-87.
24. Yang G, Lyon RF, Drakakis EM. Psychophysical evaluation of an ultra-low power, analog biomimetic cochlear implant processor filterbank architecture with across channels. AGC IEEE/ACM Trans Audi Speech Lang Process 2015;23:2465-73.
25. Qian XH, Wu YC, Yang TY, Cheng CH, Chu HC, Cheng WH, et al. Design and *In vivo* verification of a CMOS bone-guided cochlear implant microsystem. IEEE Trans Biomed Eng 2019;66:3156-67.
26. Khan SP, Auner GG, Palyvoda O, Newaz GM. Biocompatibility assessment of next generation materials for brain implantable microelectrodes. Mater Lett 2011;65:876-9.
27. Weiland JD, Anderson DJ, Humayun MS. *In vitro* electrical properties for iridium oxide versus titanium nitride stimulating electrodes. IEEE Trans Biomed Eng 2002;49:1574-9.
28. Lee CF, Li GJ, Wan SY, Lee WJ, Tzen KY, Chen CH, et al. Registration of micro-computed tomography and histological images of the guinea pig cochlea to construct an ear model using an iterative closest point algorithm. Ann Biomed Eng 2010;38:1719-27.
29. Li ML, Lee LC, Cheng YR, Kuo CH, Chou YF, Chen YS, et al. A novel aerosol-mediated drug delivery system for inner ear therapy: Intratympanic aerosol methylprednisolone can attenuate acoustic trauma. IEEE Trans Biomed Eng 2013;60:2450-60.